Influence of magnetic interaction on lattice dynamics of FeBO$_3$

View the article online for updates and enhancements.

Influence of magnetic interaction on lattice dynamics of $FeBO_3$

K. Parlinski[1], J. Łażewski[1], P. T. Jochym[1], A. Chumakov[2],
R. Rüffer[2] and G. Kresse[3]

[1] *Institute of Nuclear Physics - ul. Radzikowskiego 152, 31-342 Kraków, Poland*
[2] *European Synchrotron Radiation Facility (ESRF)*
B.P. 220, F-38043 Grenoble Cedex, France
[3] *Institute for Materials Physics, University of Vienna*
Sensengasse, 8/12, A-1090 Vienna, Austria

Abstract. – The lattice dynamics of the antiferromagnetic $FeBO_3$ crystal has been cal-
culated by *ab initio* density-functional theory and measured by nuclear inelastic absorption
spectroscopy. The calculations for the antiferromagnetic phase reproduce the experimental lat-
tice parameters of the unit cell and provide phonon dispersion relations which agree well with
the measured partial density of phonon states for the Fe atoms. Calculations for the nonmag-
netic configuration lead to a smaller crystal volume and drastically higher phonon frequencies
for the Fe atoms.

The lattice dynamics of crystals are usually considered to be independent of magnetic
properties. The influence of the magnetic structure on the phonon spectra for nonmetallic
systems, if not neglected entirely, is treated as a next-order perturbation. This assumption
is partly supported by studies of magnetic phase transitions, where the crystal structure
usually does not experience abrupt changes going from the magnetic to the paramagnetic state.
However, at the magnetic phase transitions one assumes an equilibrium between magnetic and
paramagnetic phases, therefore a similarity of their dynamical properties in a transition point
should be expected *a priori*. Indeed, the mean-square displacement mesured in the Mössbauer
effect [1], the slope of acoustic phonons and phonon frequencies themselves [2] of bcc iron do
not undergo abrupt changes across the magnetic-paramagnetic phase transition. Therefore,
much more appropriate would be an investigation of the role of the magnetic interaction on
the lattice dynamics by comparing the differences between magnetic and nonmagnetic states
directly. An obvious difficulty of such an experiment is the absence of a nonmagnetic counter-
part, *i.e.* a sample being nonmagnetic. However, the present state of the density functional
theory allows one to address the problem theoretically. Namely, in the magnetic state the *ab
initio* calculations treat the spin-up and spin-down electronic bands as independent variables,

and its difference specifies magnetic properties. In the nonmagnetic treatment the spin-up and spin-down bands are considered identical, thus preventing to create the magnetic moment in the system. We remind that the paramagnetic state loses the macroscopic magnetization due to thermal fluctuations, but the magnetic contribution to the system interaction still exists in it.

In this article, we report on *ab initio* calculations of the lattice dynamics of the ferric borate $FeBO_3$ crystal for both the magnetic and the nonmagnetic states. Contrary to common expectation, the calculations reveal a very strong influence of the magnetic structure on the lattice vibrations: the magnetic interaction reduces the mean phonon frequencies of the magnetic Fe atoms by as much as 46%. To our best knowledge, these are the first lattice dynamics calculations where accounting for the magnetic interactions resulted in such a drastic change of the vibrational frequencies. The calculations were confirmed by measurements of the partial density of phonon states for the iron atoms, performed using nuclear inelastic absorption of synchrotron radiation.

Iron borate is a weak ferromagnet with a Néel temperature of $T = 348$ K. It exists in a rhombohedral phase with the space group $R\bar{3}c$ (D_{3d}^6) ($Z = 2$), and lattice constants of $a_r = 5.520$ Å and $\alpha = 49.54°$ [3]. The magnetic moments of both Fe atoms reside in the basal symmetry plane (perpendicular to the three-fold symmetry axis), and are almost antiparallel to each other, with a small canting angle of about $1°$. A resulting small magnetic moment stays in the basal symmetry plane [4]. The $FeBO_3$ shows the magneto-optic effect.

The present *ab initio* calculations of $FeBO_3$ were performed within density functional theory, using the ultrasoft pseudopotential method [5] with the generalized gradient approximation (GGA) implemented in the VASP package [6,7]. Vanderbilt-type ultrasoft pseudopotentials, provided by the package, were used for Fe, B and O atoms. These pseudopotentials represent $3d^74s^1$, $2s^22p^1$ and $2s^22p^4$ as valence electrons, respectively. We have used the primitive rhombohedral $(\boldsymbol{a}, \boldsymbol{b}, \boldsymbol{c})$ and an enlarged $(\boldsymbol{b}+\boldsymbol{c}-\boldsymbol{a},\ \boldsymbol{c}+\boldsymbol{a}-\boldsymbol{b},\ \boldsymbol{a}+\boldsymbol{b}-\boldsymbol{c})$ supercells containing 10 and 40 atoms, respectively. The Brillouin zone integration was confined to 4 and 1 (Γ) special points, respectively. Tests with a larger number of wave vectors showed very little changes of the total energy. The nonmagnetic (NM), and the ferromagnetic (FM) and antiferromagnetic (AFM) structures with magnetic moments on the Fe atoms were considered. The lattice constants and the ground-state energies found for the primitive supercell are given in table I. The AFM configuration has the lowest ground-state energy. The FM and NM structures have slightly higher energies.

The phonon dispersion relations of $FeBO_3$ were determined by the direct method [8,9], using the enlarged and optimized supercell with 40 atoms. The Hellmann-Feynman forces were computed for x, y (along the the basal plane) and z (along three-fold symmetry axis) independent displacements of one Fe, B or O atom. The displacement amplitudes were 0.03 Å. All nine displaced configurations generate $9 \times 3 \times 40 = 1080$ components of Hellmann-Feynman

TABLE I – *Lattice parameters, magnetic moments μ and excess of the ground-state energy $\Delta E = E - E_{NM}$ per unit cell calculated for the rhombohedral $FeBO_3$ crystal. The measured lattice constants are $a = 5.520$ Å, $\alpha = 49.54°$ [4].*

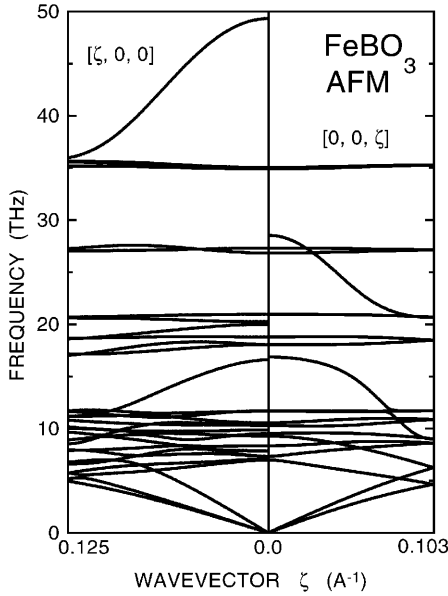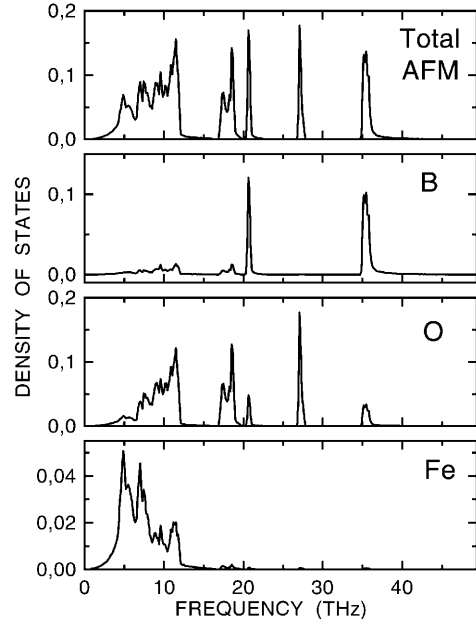| Phase	a (Å)	α (degrees)	μ (μ_B)	ΔE (eV/u.c.)
NM	5.265	50.60	0.0	0.0
FM	5.583	49.34	4.10	-1.149
AFM	5.567	49.46	± 4.08	-1.493

Fig. 1

Fig. 2

Fig. 1 – Phonon dispersion relations of the AFM phase along two crystallographic directions.

Fig. 2 – Total and partial phonon density of states for B, Fe and O atoms calculated for the AFM phase.

forces. Within this supercell there are 39 force constant matrices with 258 independent parameters. Using the PHONON program [10] the force constant parameters were fitted to Hellmann-Feynman forces. The direct method, applied to 40 atoms supercell, gives exact phonon frequencies at the Γ and F points. The values of the force constants decrease from the center to the supercell surface by three orders of magnitudes which is fast enough to describe phonon branches accurately.

In $FeBO_3$ the infrared active optical modes split into transverse (TO) and longitudinal (LO) components. The TO phonon frequencies are calculated within the direct method, while LO modes cannot be evaluated so easily. The LO modes depend on a nonanalytical term [11], which generally depends on the ratio of the effective charge tensor to the square root of the dielectric constant $\boldsymbol{Z^*}_i/\sqrt{\epsilon_\infty}$. The Berry-phase approach [12] has been used to calculate the effective charges. The calculated nonzero elements are: $Z_{xx}(B) = Z_{yy}(B) = 3.739$, $Z_{zz}(B) = 0.93$, $Z_{xx}(Fe) = Z_{yy}(Fe) = 4.589$, $Z_{zz}(Fe) = 4.89$, $Z_{xx}(O) = -2.411$, $Z_{yy}(O) = -3.141$, $Z_{zz}(O) = -1.94$ and $Z_{xz}(O) = 1.00$. We have used the measured highest frequency of the infrared active mode [13] to estimate the dielectric constant to be $\epsilon_\infty = 2.2$. These values were introduced to the analytical term added to the dynamical matrix.

For the AFM phase the calculated phonon dispersion curves are shown in fig. 1, and the irreducible representations of Γ modes are given in table II. The optic phonon branches are relatively flat confirming that the interaction range in $FeBO_3$ is rather short. Branches with large dispersions belong to infrared active modes, which are split at the Γ point. Branches with LO splitting are dominated mainly by B and O vibrations.

Figure 2 shows the total and the partial phonon density of states. The first one spreads over a large frequency range from 0 up to 49 THz. The Fe atoms vibrate together with oxygen

TABLE II – *Calculated frequencies (in THz) of the zone-center modes of the nonmagnetic (NM) and antiferromagnetic (AFM) phases of* $FeBO_3$. *For the NM phase we give the phonon frequencies corresponding to TO modes only. In the AFM and IR columns the two frequencies denote LO/TO modes. The* R *and* I *indices correspond to Raman and infrared active modes, respectively. The infrared measurements* IR1 *and* IR2 *refer to* [13] *and* [14], *respectively. Raman modes are taken from ref.* [15].

Mode	AFM	IR1	IR2	Raman	NM
E_u(I)	6.98/7.08	–	6.95	–	10.68
E_g(R)	7.33	–	–	8.37	9.20
A_{2u}(I)	7.86/11.67	–	8.33	–	11.86
E_u(I)	8.34/9.86	–	8.05	–	11.43
A_{2g}	9.28	–	–	–	12.76
A_{1u}	9.52	–	–	–	11.26
E_g(R)	10.28	–	–	12.0	13.74
E_u(I)	10.55/16.58	–	11.69	–	16.90
A_{2g}	11.67	–	–	–	14.29
A_{2u}(I)	11.71/16.86	–	13.67	–	15.48
E_g(R)	18.05	–	–	19.3	19.38
E_u(I)	18.78/19.99	19.9	19.67	–	20.64
A_{2u}(I)	20.24/28.53	–	22.78	–	20.43
A_{2g}	20.95	–	–	–	20.72
A_{1g}(R)	26.83	–	–	27.7	27.60
A_{1u}	27.30	–	–	–	28.71
E_g(R)	34.90	–	–	36.3	35.27
E_u(I)	35.03/49.32	36.3/49.0	35.96	–	36.24

atoms in the lower frequency range. The B atoms occupy, in practice, two frequencies only. The O atoms take part in all vibrations, but there is one mode at 27 THz, which belongs exclusively to oxygen motion.

The calculations were compared with experimental data obtained with nuclear inelastic spectroscopy, which gives a direct access to the partial density of states of the Fe atoms [16], whereas neutron inelastic experiment would be difficult because of the numerous vibration modes (fig. 1) and strong boron absorption. Energy spectra of nuclear inelastic absorption were measured at the Nuclear Resonance beam line [17] at the ESRF. A single crystal of $^{57}FeBO_3$ with 95% abundance in the resonant ^{57}Fe isotope was used. Compared to earlier studies [18], we utilized the best available energy resolution (0.16 THz), which is mandatory for a proper comparison with the calculations. Spectra of nuclear inelastic absorption were measured at room temperature (294 K) in two geometries: almost along the basal plane (5° deviation) and along the three-fold symmetry axis. From these data the partial Fe density of phonon states along the corresponding directions were derived. Detailed discussion of the method can be found elsewhere [17].

In fig. 3 we compare the partial density of states for Fe atoms within our DFT-GGA calculations for the AFM phase with measurements of nuclear inelastic absorption. The overall agreement is very good. For vibrations along the three-fold symmetry axes the calculations reproduce nicely the two pronounced phonon peaks at 4.8 and 6.4 THz. Note that the peak at 4.8 THz is reflecting mainly the zone boundary modes.

In order to evaluate the influence of the magnetic interactions on the lattice dynamics, we
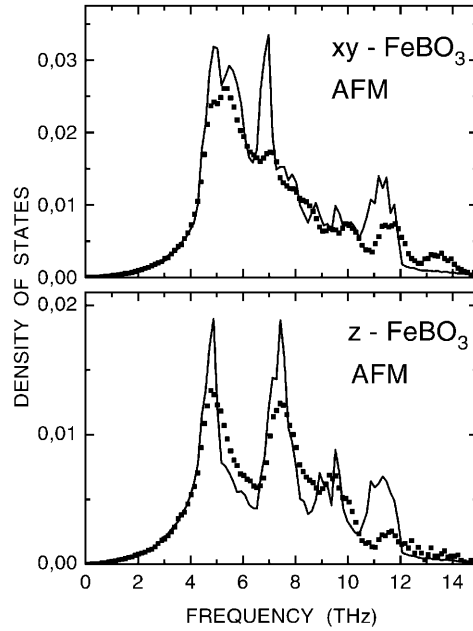
Fig. 3 – Comparison of the partial phonon density of states for Fe atoms calculated for the AFM phase (solid line) and measured by nuclear inelastic absorption (squares). Top: vibrations along basal plane. Bottom: vibrations along the three-fold symmetry axis.
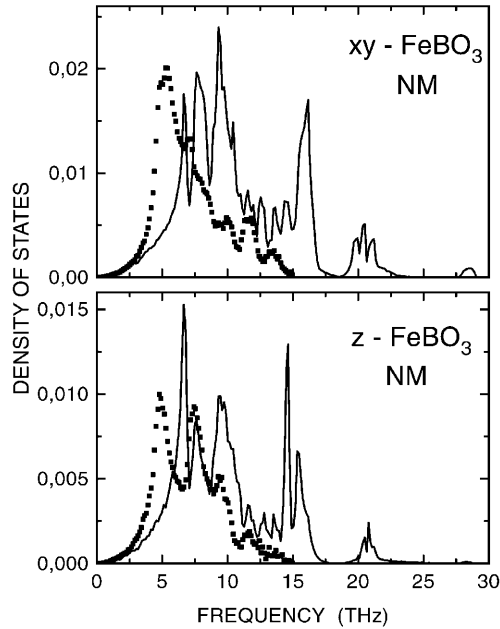

Fig. 4 – Comparison of the partial phonon density of states for Fe atoms calculated for the NM phase (solid line) and measured for the AMF phase by nuclear inelastic absorption (squares). Top: vibrations along the basal plane. Bottom: vibrations along the three-fold symmetry axis. Notice the different frequency interval compared to fig. 3.

have calculated the partial Fe phonon density of states for the nonmagnetic phase (not existing in reality). Figure 4 compares the calculations for the NM phase with the same experimental data for both geometries. A drastic difference is clearly seen. The calculated phonon spectrum is expanded by about 46% towards higher frequencies. The total density of states for the NM phase (not shown) revealed that this expansion concerns mainly the Fe atoms. The B and O atom vibrations are relatively insensitive to the magnetic interaction. The drastic change of the phonon spectrum for Fe atoms results mainly from a decrease of the lattice constant and a decrease of the unit cell volumes from $V_{\mathrm{AFM}} = 30.53$ Å^3 to $V_{\mathrm{NM}} = 26.76$ Å^3. To verify this, we repeated the calculations for NM state at a volume $V = 30.53$ Å^3. This configuration remains stable when applying a negative pressure of -22.6 GPa. At this strained NM state the mean frequency of the Fe phonon density of states increased by only 15%. Thus, larger interatomic distances in AFM phase cause smaller atomic forces and, consequently, a decrease of phonon frequencies.

In summary, we have performed a detailed analysis of the lattice dynamics in FeBO$_3$ and found a very strong influence of the magnetic interaction on the phonon spectrum of the magnetic Fe atoms. *Ab initio* calculations of the AFM phase reproduce properly the lattice parameters of the unit cell and give dispersion relations which agree well with the partial Fe density of phonon states measured by nuclear inelastic absorption. In contrast, calculations of the NM phase give a 12% smaller volume for the unit cell and 46% higher mean frequency vibrations of magnetic atoms. Thus the antiferromagnetic interaction between the Fe atoms enlarges the rhombohedral unit cell in the FeBO$_3$ crystal and lowers the vibration frequencies of the magnetic atoms. To our knowledge, such a strong influence of the magnetic interaction on the lattice dynamics was not yet reported.

$$* * *$$

REFERENCES

[1] KOLK B., BLELOCH A. L. and HALL D. B., *Hyperfine Interact.*, **29** (1986) 1377.
[2] SATIJA S. K., COMÉS R. P. and SHIRANE G., *Phys. Rev. B*, **32** (1985) 3309.
[3] DIEHL R., *Solid State Commun.*, **17** (1975) 743.
[4] DIEHL R., JANTZ W., NOLÄNG B. I. and WETTLING W., *Growth and properties of iron borate, FeBO,3*, in *Current Topics in Materials Science*, edited by KALDIS E., Vol. **11** (Elsevier Science Publishers B.V.) 1984, p. 241.
[5] VANDERBILT D., *Phys. Rev. B*, **41** (1990) 7892; PASQUARELLO A., LAASONEN K., CAR R., LEE C. and VANDERBILT D., *Phys. Rev. Lett.*, **69** (1992) 1982; LAASONEN K., PASQUARELLO A., CAR R., LEE C. and VANDERBILT D., *Phys. Rev. B*, **47** (1993) 10142.
[6] KRESSE G. and FURTHMÜLLER J., Software VASP, Vienna (1999); *Comput. Mat. Sci.*, **6** (1996) 15; *Phys. Rev. B*, **54** (1996) 11169.
[7] KRESSE G. and HAFNER J., *Phys. Rev. B*, **47** (1993) 558; **49** (1994) 14251.
[8] KRESSE, G. FURTMÜLLER J. and HAFNER J., *Europhys. Lett.*, **32** (1995) 729.
[9] PARLINSKI K., LI Z. Q. and KAWAZOE Y., *Phys. Rev. Lett.*, **78** (1997) 4063; *Phys. Rev. B*, **61** (2000) 272.
[10] PARLINSKI K., Software PHONON (2000).

[11] Pick R. M., Cohen M. H. and Martin R. M., *Phys. Rev. B*, **1** (1970) 910; Maradudin A. A., *Elements of the Theory of Lattice Dynamics*, in *Dynamical Properties of Solids*, edited by Horton G. K. and Maradudin A. A., Vol. **1** (North-Holland Publishing Company, Amsterdam) 1974, p. 3.

[12] Vanderbilt D. and King-Smith R. D., *Phys. Rev. B*, **48** (1993) 4442.

[13] Infrared spectrum has been measured in the 12–60 THz frequency range using Bruker IFS28 spectrometer with 0. 06 THz resolution. Private communication from Le Quéré A.-M. (ESRF).

[14] Wakamura K., Okuda T. and Tsushima T., *Opt. Commun.*, **23** (1970) 249.

[15] Shepherd I. W., *Phys. Rev. B*, **5** (1972) 4524.

[16] Seto M., Yoda Y., Kikuta S., Zhang X. W. and Ando M., *Phys. Rev. Lett.*, **74** (1995) 3828; Sturhahn W., Toellner T. S., Alp E. E., Zhang X. W., Ando M., Yoda Y., Kikuta S., Seto M., Kimball C. W. and Dabrowski B., *Phys. Rev. Lett.*, **74** (1995) 3832.

[17] R. Rüffer and Chumakov A., *Hyperfine Interact.*, **97/98**, (1996) 589; **113** (1998) 59.

[18] Chumakov A. I., Rüffer R., Baron A. Q. R., Grünsteudel H., Grünsteudel H. F. and Kohn V. G., *Phys. Rev. B*, **56** (1997) 10758.